Available online at www.sciencedirect.com
ScienceDirect
European Journal of Medicinal Chemistry 41 (2006) 1231–1239
EUROPEAN JOURNAL OF MEDICINAL CHEMISTRY
http://france.elsevier.com/direct/ejmech

Original article

Nitrofurylsemicarbazone Rhenium and Ruthenium Complexes as Anti-trypanosomal Agents

Lucía Otero[a], Gabriela Aguirre[b], Lucía Boiani[b], Ana Denicola[c], Carolina Rigol[d], Claudio Olea-Azar[d], Juan Diego Maya[e], Antonio Morello[e], Mercedes González[b], Dinorah Gambino[a,*], Hugo Cerecetto[b,*]

[a] *Cátedra de Química Inorgánica, DEC, Facultad de Química, Universidad de la República, Montevideo, Uruguay*
[b] *Departamento de Química Orgánica, Facultad de Química – Facultad de Ciencias, Universidad de la República, Montevideo, Uruguay*
[c] *Laboratorio de Fisicoquímica Biológica, Facultad de Ciencias, Universidad de la República, Montevideo, Uruguay*
[d] *Departamento de Química Inorgánica y Analítica, Facultad de Ciencias Químicas y Farmacéuticas, Universidad de Chile, Santiago, Chile*
[e] *Departamento de Farmacología Clínica y Molecular, Facultad de Medicina, Universidad de Chile, Santiago, Chile*

Received in revised form 11 May 2006; accepted 18 May 2006
Available online 07 July 2006

Abstract

Rhenium and ruthenium complexes of the type $[Re^{V}OCl_2(PPh_3)L]$ and $[Ru^{II}Cl_2(DMSO)_2L]$, where L are 5-nitrofurylsemicarbazone derivatives, were prepared in an effort to obtain new anti-trypanosomal agents combining the recognized biological activity of these metals and the trypanocidal activity of the free ligands. Rhenium complexes resulted unstable in aqueous solution not allowing their use as potential drugs. On the other hand, complexation to ruthenium of the bioactive ligands lead to the lack of antiprotozoa activity even though free radical production and redox cycling induction were detected when the compounds were incubated in presence of *Trypanosoma cruzi* cells. The lack of anti-trypanosomal activity of ruthenium complexes could be explained on the basis of their high protein binding capacity and their high hydrophilicity.

Keywords: Rhenium complexes; Ruthenium complexes; Anti-trypanosomal activity

1. Introduction

Chagas' disease or American trypanosomiasis is an important health problem that affects around twenty million people in Central and South America. 2–3 Million individuals develop the typical symptoms of this disease that results in 50 000 yearly deaths [1,2]. The causative agent of this disease is the haemoflagellate protozoan *Trypanosoma cruzi* (*T. cruzi*), which is transmitted to humans and other mammals, in rural areas, by reduviid bugs such as *Rhodnius prolixus* and *Triatoma infestans* [3]. Current pharmacological treatment has been based on benznidazole (a nitroimidazole derivative) and nifurtimox (a nitrofuran derivative, Nfx, Fig. 1), compounds that cause significant side effects and show poor clinical efficacy [4–6]. These two drugs are effective against the circulating form of the parasite (trypomastigote) during the acute phase of the disease, but not during the chronic stage. Therefore, there is an urgent need for the development of effective agents acting at key targets in *T. cruzi*.

The last decades have seen a growing interest in transition metal complexes as potential antineoplastic agents [7]. Some promising results have been obtained with derivatives of different metals, like Pt, Ti, Rh, Au and Ru. In particular, several ruthenium complexes have exhibited good to excellent anti-tumor activity in some tumor screens and Ru(II) complexes containing imidazole ligands have shown antimetastatic activity against some murine tumor models [8]. DNA has been recognized as the main target for Ru drugs although it has been claimed that DNA-independent mechanisms are also responsible for their anti-tumor activity. On the other hand, a good correlation between antitumor and trypanostatic properties of several metal-based drugs has been observed. This is probably attributable to biochemical similarities between tumor cells and pathogenic trypanosomes in terms of metabolism and lack of protecting enzymes like catalases and perox-

* Corresponding authors.
E-mail addresses: dgambino@fq.edu.uy (D. Gambino), hcerecet@fq.edu.uy (H. Cerecetto).

0223-5234/$ - see front matter © 2006 Published by Elsevier Masson SAS.
doi:10.1016/j.ejmech.2006.05.012

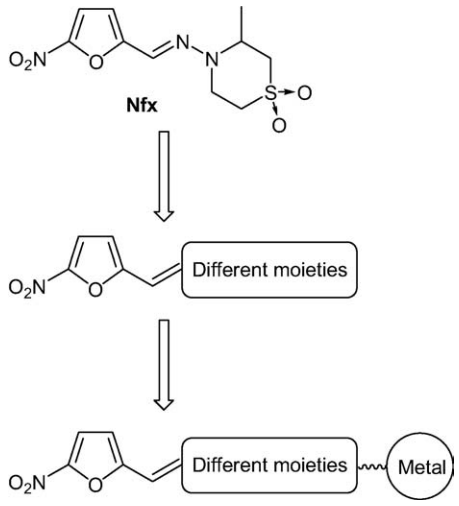

Fig. 1.

idases [9,10]. In this sense, the synthesis of metal complexes with ligands bearing activity could be a promising approach towards the development of new agents against protozoa. Previous work has shown that some metal complexes of certain anti-trypanosomal drugs (imidazole and thiazole derivatives) resulted to be more active than the corresponding free ligands [11–15]. In addition, this approach has also been successfully used in the development of new agents against other protozoa such as *P. falciparum* [16] and *E. histolytica* [17–19].

Several types of organic compounds have been described as anti-*T. cruzi* agents. As part of our current research program, 5-nitrofuryl derivatives have been synthesized and biologically evaluated as antichagasic agents. Among them semicarbazone and thiosemicarbazone derivatives have shown good anti *T. cruzi* activity [20–25].

In our previous studies, we have incorporated the 5-nitrofuryl pharmacophore and a potentially active metal (Re or Ru) in the same molecule, in order to obtain complexes with a potential dual mechanism of cytotoxic action (derivatives **5-9**, Fig. 1 and Fig. 2) [26,27].

In this work, a new ruthenium complex **10** with the N^4-butyl derivative of 3-(5-nitrofuryl)acroleine semicarbazone as ligand (**4**) has been synthesized and fully characterized. In addition, the ability of both series of Re and Ru complexes to inhibit *T. cruzi* growth was tested (Fig. 2). Biological behavior, including intra-parasite free radical production, parasitic respiration inhibition, complexes' stability and protein-binding capacity, was also investigated.

2. Chemistry

The semicarbazone moiety, having suitable donor atoms, allowed us to include the Re or Ru atom and the 5-nitrofuryl pharmacophore in the same molecule. Semicarbazones **1-4** [20,28] (Fig. 2) resulted interesting tools for the development of the desired compounds, due to their different electronic and lipophilic properties that could lead to different biological responses. As previously reported, rhenium complexes **5** and **6** were obtained by reaction of one equivalent of the precursor $[Re^{V}OCl_3(PPh_3)_2]$ [29] with two equivalents of **1** or **2** in ethanol (for derivatives **5**) or methanol (for derivative **6**) under reflux, through a ligand substitution reaction where one PPh_3 molecule and a Cl atom act as leaving groups [26]. Ruthenium complexes **7-9** were obtained by reaction of one equivalent of the precursor $[Ru^{II}Cl_2(DMSO)_4]$ [30] with two equivalents of **1**, **2**, or **3** in ethanol (for derivatives **7** and **8**) or toluene (for derivative **9**) under reflux, through a ligand substitution reaction where two DMSO molecules act as leaving groups [27]. Complexes were identified by microanalysis (C, H, N, S), FAB-MS, IR and electronic spectroscopies, ^{1}H NMR, ^{13}C NMR and HETCOR experiments. In addition, crystal and molecular structure of derivatives **5**, **7** and **9** were determined

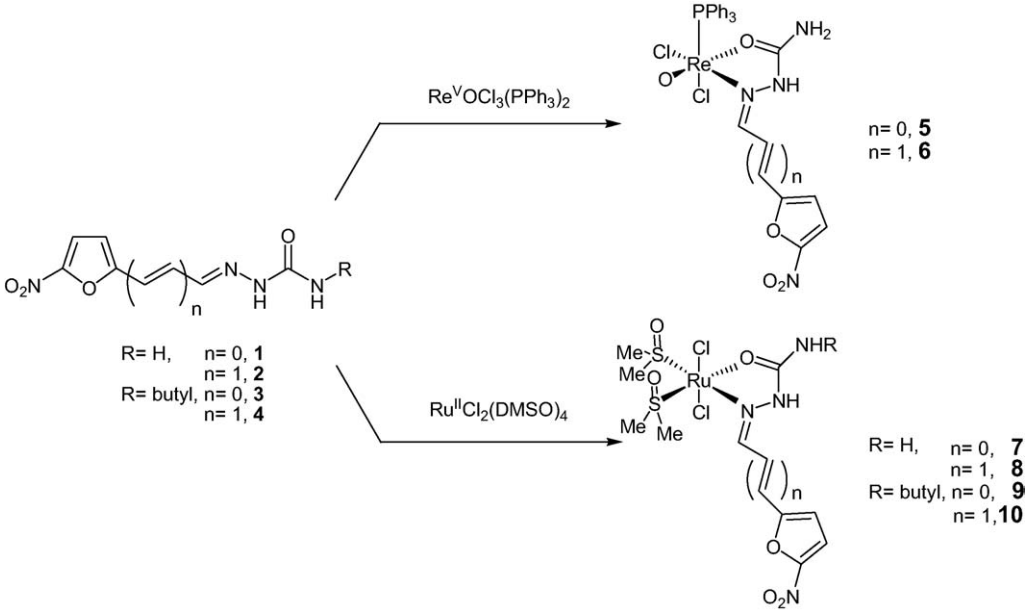

Fig. 2.

by X-ray diffraction methods [26,27]. In this work, a new ruthenium complex (**10**) with **4** as ligand was obtained by a similar procedure and fully characterized. New ruthenium derivative **10** was prepared in good yields and high purity. Elemental analyses and FAB-MS results are in accordance to the proposed formulae. Significant vibration bands of the ligand and the metal complex, useful for determining the ligand's mode of coordination, could be tentatively assigned. After coordination, the ν(CO) and the ν(C=N) bands of the semicarbazone free ligand, at 1670 cm^{-1} and 1578 cm^{-1} respectively, shift to lower frequencies (1640 cm^{-1} and 1519 cm^{-1}, respectively). These modifications are consistent with bidentate coordination of the semicarbazone ligand through the carbonylic oxygen and the azomethynic nitrogen. The ν(NH) band at ca. 3120 - 3150 cm^{-1} is present in the complex, indicating that, in the solid state, the ligand remains protonated. In addition, the ν (SO) band, observed at 1108 cm^{-1}, confirms the presence of sulfur-bonded DMSO in the Ru coordination sphere [26,27]. The NMR experiments show narrow signals, typical for Ru (II) diamagnetic complexes. HETCOR experiments allowed to assign all signals of the free ligands and the investigated complexes ^{1}H NMR integrations and signal multiplicities are also in agreement with the proposed formula. The new complex shows similar ^{1}H and ^{13}C chemical shifts to the previously reported ruthenium nitrofurylsemicarbazone complexes [26,27].

3. Pharmacology

3.1Anti-protozoal Activity

The trypanocidal activity of all complexes was tested in vitro against *T. cruzi*, Tulahuen 2 strain, as previously described [31]. The compounds were incorporated into the medium at different concentrations. Percentage of growth inhibition (PGI) was evaluated in comparison to the control (no drug added to the medium) at day 5. Nfx was used as the reference trypanocidal drug (Table 1).

In order to study the effect, on the observed activity, of complex-protein interaction in the culture medium, trypanocidal activity of the ruthenium complex **7** in the absence of culture medium was studied. The parasites were incubated during 5 h in buffer solution and in the presence of different concentrations of selected compound. After that 5 h incubation, cells were harvested and then were grown in BHI-Tryptose, complemented with 5% fetal bovine serum medium and the PGI were determined at day 5 (Table 1).

3.2. Stability of the Complexes in Aqueous Medium

The stability of rhenium complexes **5** and **6** was followed at 10^{-4} M in 1% DMSO, 100 mM phosphate buffer, pH=7.4 at 28 °C using electronic spectroscopy in the visible region. Release of the ligands **1** and **2** was detected immediately after dissolution of the complexes. The absence of bands in the visible region of the electronic spectra (except those of the ligands) suggests the oxidation of the complexes to ReO_4^- in such conditions, with the concomitant release of the semicarbazone ligand.

The stability of ruthenium complexes **7-10** was followed for 48 h, at 10^{-4} M in 0.5% DMSO, 100 mM phosphate buffer, pH=7.4 at 28 °C using electronic spectroscopy in the visible region and conductivity measurements. The spectroscopic studies showed the displacement of the absorption maximum of the complexes, at around 450 nm, to lower wavelengths and the presence of an isosbestic point (Fig. 3a). These results suggest a very slow single chloride substitution process by water. In addition, conductivity measurements showed that the number of ions in solution increased with time indicating that the hydrolytic process, as expected, lead to charged species (Fig. 3b). Only after three days, a partial release of the free ligands was detected through the appearance of the corresponding band at *c.a.*

Table 1
In vitro anti-*T. cruzi* behaviour

	Ligands		Rhenium complexes		Ruthenium complexes	
	Compd.	PGI (%) [a,b] (doses, μM)	Compd.	PGI (%) [a,b] (doses, μM)	Compd.	PGI (%) [a,b] (doses, μM)
Assay in axenic medium	**1**	78 (5)	**5**	65 (5)	**7**	0 (5)
		96 (15)		80 (15)		11 (15)
		100 (25)		92 (25)		–
	2	50 (5)	**6**	64 (5)	**8**	20 (5)
		90 (15)		78 (15)		44 (15)
		100 (25)		89 (25)		71 (25)
	3	25 (5)			**9**	0 (5)
		–	–	–		0 (15)
		–				0 (25)
	4	84 (5)			**10**	45 (5)
		100 (15)	–	–		63 (15)
		100 (25)				–
	Nfx	50 (5)	–	–	–	–
		100 (25)				–
Assay in buffer solution	**1**	74 (15)	–	–	**7**	43 (15)
		100 (25)				82 (25)
	Nfx	20 (15)	–	–	–	–

[a] PGI: percentage of growth inhibition.
[b] The results are the mean values of three different experiments with a SD less than 10% in all cases.

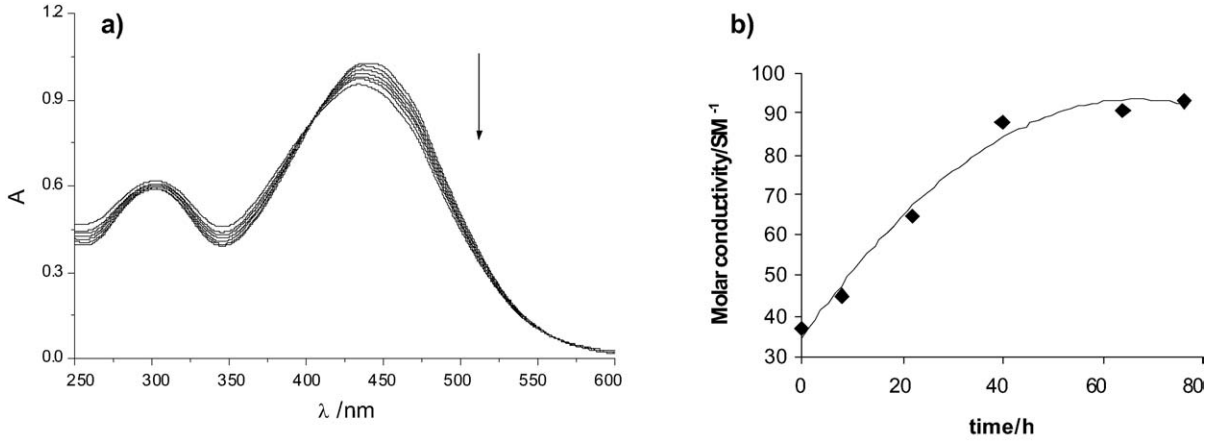

Fig. 3. **a)** Electronic spectra of compound **7** 10^{-4} M at different times, intervals = 5 h, in 100 mM phosphate buffer:DMSO (99.5:0.5). **b)** Molar conductivity of compound **7** at different times in water:DMSO (99.5:0.5).

370 nm in the electronic spectra. So, a simultaneous but much slower decomposition process is also taking place.

3.3. Electrochemical Studies

Electrochemical behavior of the ligands and the corresponding ruthenium complexes was studied. Cyclic voltammetric experiments were performed, in organic medium, in order to determine the peak potentials of the nitro moiety. Ligands **1-4** and complexes **7-10** showed similar electrochemical behavior in the reduction process.

When the potential was scanned in a negative direction, at all scan rates investigated, a peak near 0.9 V corresponding to the reduction of the nitro group was observed (Fig. 4). Table 2 lists the values of the voltammetric peaks corresponding to the nitro moiety.

3.4. Partition Coefficient Determination

The partition coefficients (P_{OW}) were determined for the ligands and the corresponding ruthenium complexes using electronic spectroscopy in the visible region, *n*-octanol as non-polar phase and physiological serum as polar one (Table 2) [33]. A drastic decrease of the measured lipophilicity is observed as a consequence of the coordination to ruthenium. Only, derivative **10** showed a P_{OW} value adequate for a potential drug [34].

3.5. Interaction with albumin

The interaction of ruthenium complexes **7-10** with bovine serum albumin (BSA) as a model protein was investigated. Complexes were incubated at 37 °C with BSA for different time periods and using different metal to protein molar ratios. After ultrafiltration, the amount of non-bound ruthenium complexes was quantified by electronic spectroscopy. The percentage of bound complex to BSA was followed with time as shown in Table 2. Clearly, compound **10** presented a different behavior in comparison to complexes **7-9**. Interaction of compound **10** with BSA seem to be faster than the ones observed for derivatives **7-9** (i.e. 50% vs. 10% after 2 h of exposure, respectively, for a 2:1 complex:BSA ratio). However, after 96 h incubation the percentage of BSA-bound to complexes **7-9** reached the maximum 100%, while remained 50% for derivative **10**.

It is important to note that the visible spectrum of metal complexes changed in the presence of BSA. In all cases, a

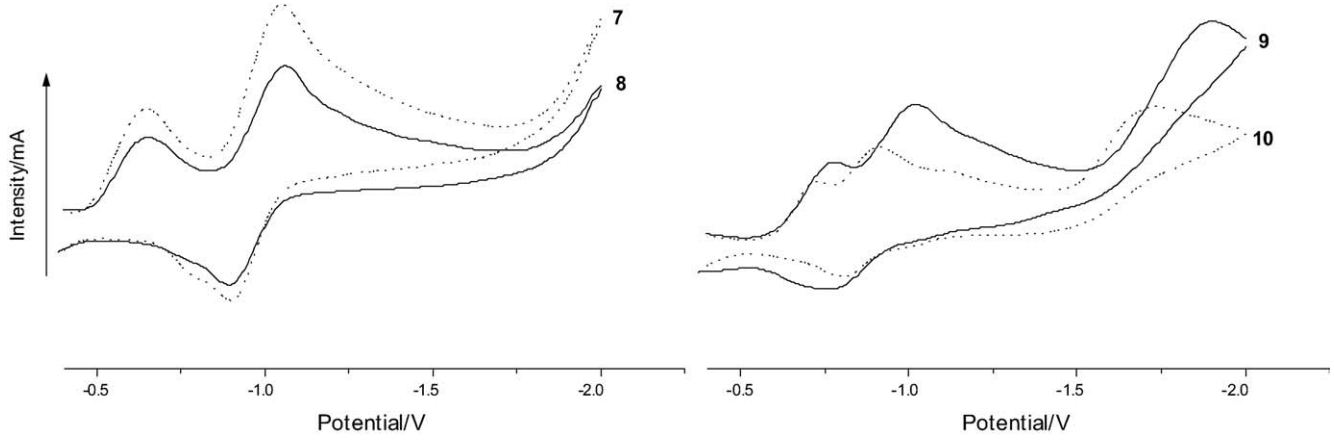

Fig. 4. Cyclic voltammograms at 25 °C of 10^{-3} M solutions of **7-10** in DMSO/0.1M (TBA)PF_6 at 2.0 V/s.

Table 2
Physicochemical characterization of developed compounds

Ligands			Complexes				
Comp.	$E_{1/2}$ [a]	P_{OW}	**Compd.**	$E_{1/2}$ [a]	P_{OW}	Binding to BSA	
						Percentage of complex bound to BSA (%) [c]	Time (h)
1	–0.87	1.93 [b]	**7**	–0.99	0.07 [b]	50	24
						100	96
2	–0.85	9.33 [b]	**8**	–0.89	0.13 [b]	50	24
						100	96
3	–0.87	2.25 [b]	**9**	–0.97	0.32 [b]	50	24
						100	96
4	–0.86	29.0	**10**	–0.92	5.80	50	2
						50	96

[a] Versus saturated calomel electrode; scan rate: 2.0 V/s.
[b] Reference [32].
[c] Molar ratio complexes:BSA = 2:1. BSA: bovine serum albumin.

clear displacement of the complexes absorption bands to higher wavelengths (*c.a.* 10-20 nm shift) after BSA interaction was observed. These results not only confirm the interaction of these complexes with the protein but also suggest a change in the ruthenium coordination sphere and thus a covalent interaction between the protein and the metal.

On the other hand, the interaction of ruthenium complex **7** with BSA did not induce fragmentation of the protein as confirmed by gel electrophoresis. Different protein:complex ratios were incubated at 37 °C for 24 hs and then run on 10% SDS-PAGE. No protein bands were detected with lower molecular weight than BSA.

3.6. Confirmation of Mechanism of Action

According to our design, the developed ruthenium complexes would act by a dual mechanism: intra-parasitic free radical production due to the ligand and DNA interaction due to the metal. Previously, we had demonstrated that these compounds were able to bind to DNA [32]. Herein, we studied, using ESR spectroscopy and biochemical methods, the ability of the compounds to produce free radicals into the parasite.

3.6.1. ESR Studies

Incubation of derivative **7** with the epimastigote form of *T. cruzi* in the presence of 5,5-dimethyl-1-pirroline-*N*-oxide (DMPO) as spin trapping agent allowed to detect free radicals generated by bio-reduction promoted by the parasite (Fig. 5) [35]. The observed pattern of the ESR signals were consistent with the trapping of both the hydroxyl radical and the nitroheterocycle radical from **7** (DMPO-OH spin adduct $a_N = a_H = 14.78$ G, (*); DMPO-**7 free radical** spin adduct $a_N = 15.21$ G, $a_H = 23.48$ G, (#)). These hyperfine constants are in agreement with the splitting constants of other DMPO-OH adducts reported and nitrogen-centered radical trapping by DMPO [36,37].

3.6.2. Oxygen uptake

The effect of ruthenium complex **7** on *T. cruzi* respiration was studied measuring the oxygen consumption by the parasite at different concentrations of the compound [38]. In order to better evaluate redox cycling, mitochondrial respiration was inhibited with 30 μM sodium cyanide. The results are gathered in Fig. 6. Compound **7** produced a dose-dependent increase of oxygen consumption that is better observed after the inhibition of mitochondrial respiration by cyanide. Similar results had been previously described for the free ligand **1** [38].

4. Discussion

Rhenium complexes, **5** and **6**, decomposed almost immediately in 1% DMSO aqueous solution (phosphate buffer, pH=7.4). These results are consistent with the fact that observed trypanocidal activities are those corresponding to the free ligands (Table 1).

All ruthenium complexes, **7-10**, had shown excellent DNA binding properties [32]. Moreover, oxygen uptake and ESR experiments demonstrate that these complexes, similarly to Nfx, could be involved in redox cycling processes generating oxidative stress in the parasite. However, these derivatives were

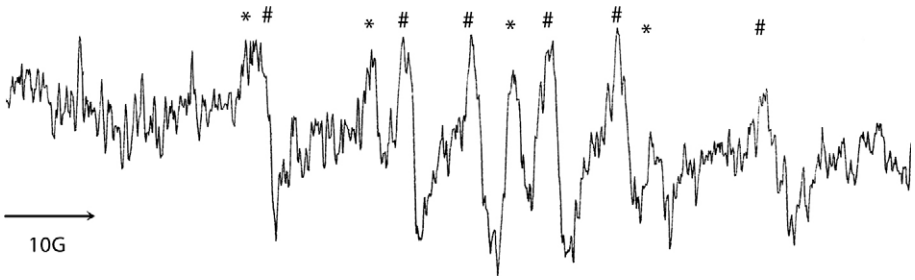

Fig. 5. *ESR spectrum obtained after 5 min incubation of *T. cruzi*–epimastigote and derivative **7**, see Experimental Section for experimental details. (*): DMPO-OH· adduct, (#): DMPO-**7 free radical** adduct.

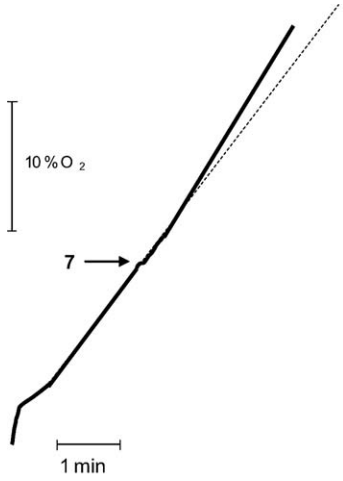

Compd.	Respiration [a]			% increase of oxygen consumption [b]			% oxygen redox cycling [c]
	150 μM	300 μM	600 μM	150 μM	300 μM	600 μM	
7	28	31	35	0	7	22	25

[a] Expressed as nanoatom of oxygen/min/mg protein.

[b] Values are expressed as percentage of control (without compound **7**) and correspond to the mean ± standard deviation of three independent experiments.

[c] Increase of oxygen consumption in the presence of NaCN (30 μM), after addition of 600 μM compound **7**.

Fig. 6. Left: Effect of compound **7** (300 μM) on the parasitic oxygen consumption. The rate of parasitic oxygen consumption changed when compound **7** was added (arrow). Right: Effect of compound **7** upon oxygen uptake *T. cruzi* (see Experimental Section for experimental details).

poor or non trypanocidal agents in the assayed conditions. At 5 μM, complexes **7-9** showed poor in vitro anti-*T. cruzi* activity even though the free ligands **1-3** resulted active (Table 1). Complex **10**, although active at 5 μM (PGI 45%), resulted less active than the corresponding ligand **4** (PGI 84%).

The physicochemical properties of the complexes could be indicative of the reasons for the previously described biological behaviour. On one hand, spectroscopic and conductimetric stability studies, under the assayed conditions showed that complexes **7-10** suffer a very slow hydrolytic process (substitution of chlorine by water in the coordination sphere) and an even slower decomposition process resulting in bioactive ligand release. However, the assayed concentrations in these stability studies were 10^2-10^3 higher (10^{-3}, 10^{-4} M) than the complexes concentration in the biological assays (10^{-6} M). So, in the bioassay conditions, the decomposition process should be even slower and thus no effect on the measured activity should be expected.

On the other hand, the redox behavior of all derivatives (**7-10**) is adequate [39] for an anti-*T. cruzi* activity. The reduction potential for the nitro moiety slightly changed when the ligand was coordinated to ruthenium, shifting – 0.04 to – 0.12 V. This moderate change could not be responsible for the great change in the biological response between ligands and complexes.

Two factors were identified as potential contributors to the low anti-*T. cruzi* activity observed of the complexes. One is the poor lipophilicity of the complexes **7-9** (Table 2). When the ligands **1-3**, with P_{OW} values ranging between 1.93 and 9.33, coordinate to ruthenium, the corresponding P_{OW} decreased drastically (0.07 to 0.32). As it is well known, the lipophilicity of a drug plays a significant role in numerous biological responses [33]. These complexes resulted 10 to 100 times more hydrophilic than the parent ligands, and thus its transport through the cell membrane could be compromised. Otherwise, complex **10** presented an adequate P_{OW} (5.80) that is in agreement with the better biological behavior of this complex. Second, the complexes ability to bind proteins could be playing an important role in the poor displayed activity. This is clearly stated by the fact that even though compound **7** showed no activity in the regular anti-*T. cruzi in vitro* assay, when the experiment was performed in the absence of proteins (no culture media) the compound displayed an acceptable level of *T. cruzi* cytotoxicity (see Table 1). In the performed BSA interaction studies, it was clear that complexes **7-9** bind to the protein in a different manner than does derivative **10** (Table 2). For the former, binding to protein was slow but complete after long incubation periods (four days). For derivative **10**, binding to BSA was fast but only 50% of complex bound, indicating less binding sites in BSA for this complex. These observations are in agreement with the biological behavior of the complexes **7-10** in the anti-*T. cruzi* assays. But, moreover, they are also in accordance to the previously reported lack of antitumor activity of these ruthenium complexes in spite of their high DNA interaction levels [32]. Strong interaction of other Ru(III) complexes with serum proteins have been reported [40] and the protein-bound complex exhibited higher antitumoral activity. Binding to proteins can result in dramatic change of the protein structure leading to protein disfunction that could be part of the cytotoxic effect. But also, binding to proteins might result into modifications or even loss of biological activity of the metal complex. This work confirms that Ru complexes **7-10** strongly interact with BSA yielding significantly less active trypanocidal compounds.

5. Conclusions

The results presented above indicate that the developed ruthenium complexes could be a good starting point for further chemical modification in order to improve the anti-*T. cruzi* activity of the selected ligands.

The information obtained in this work provides a guide to design more lipophilic ruthenium complexes with this family of ligands, which could show the desired activity maintaining or improving the oxidative stress properties and the DNA binding levels. Synthetic attempts in this direction are currently in progress.

6. Experimental protocols

6.1. Chemistry

Reagents and compound **1** were commercially available research-grade chemicals and were used without further purification. Ligands **2-4**, $[Re^{V}OCl_3(PPh_3)_2]$, $[Ru(II)Cl_2(DMSO)_4]$ and complexes **5-9** were prepared as previously reported [20, 26–30]. For the organic procedures the solvents were dried and distilled prior to use, and the reactions were carried out in a nitrogen atmosphere. Elemental analyses were performed on a Carlo Erba EA 1108 CHNS-O analyzer. Infrared spectra were recorded on a Perkin Elmer 1310 or a Bomen MB 102 apparatus in the range 4000-400 cm^{-1}, using potassium bromide tablets. Routine FAB+ spectra of the metal complexes have been measured with a TSQ spectrometer (Finnigan) with nitrobenzylalcohol as matrix. The ion gun was operated at 8 kV and 100 μA (probe temperature: 30 °C). Xenon was used as primary beam gas. ^{1}H-NMR, ^{13}C-NMR spectra and HETCOR experiments were recorded on a Bruker DPX-400 (at 400 MHz and 100 MHz) instrument.

6.1.1. $[RuCl_2(DMSO)_2$ 4], 10

$[Ru^{II}Cl_2(dmso)_4]$ (100 mg, 0.21 mmol) and **4** (59 mg, 0.21 mmol) were heated under reflux in ethanol (10 mL) during 8-10 hours, after which a solid precipitated. The solid was filtered off and recrystallized from methanol. Red solid, yield 60%. Calcd. ($C_{16}H_{27}Cl_2N_4O_6S_2Ru$) (%): C 31.6, H 4.4, N 10.8, S 10.5; found C 31.9, H 4.7, N 10.9, S 10.4. *m/z* (EI) 610 ($M^{+\cdot}$), 573 ($M^{+\cdot}$ - Cl), 530 ($M^{+\cdot}$ - DMSO), 495 ($M^{+\cdot}$ – DMSO - Cl) and 452 ($M^{+\cdot}$ – 2 DMSO). UV (acetone): $\lambda_{máx} = 465$ nm ($\varepsilon = 1.\ 2 \times 10^3\ M^{-1}cm^{-1}$). IR (KBr), ν: 1640 (CO), 1519 (C=N), 1350 (ν_s NO_2), and 1108 (SO) cm^{-1}. δ_H(acetone-d_3) 0.94 (t, 3H, CH_3), 1.42 (m, 2H, CH_2), 1.61 (m, 2H, CH_2), 3.37 (s, 6H, DMSO-CH_3), 3.38 (s, 6H, DMSO-CH_3), 3.43 (q, 2H, NCH_2), 7.03 (bt, 1H, NH), 7.15 (d, 1H, CH=), 7.18 (d, 1H, H-furane), 7.49 (dd, 1H, CH=), 7.63 (d, 1H, H-furane), 9.17 (d, 1H, CH=N), and 11.05 (bs, 1H, NH). δ_C(acetone-d_3) (HMQC, HMBC) 13.51 (CH_3), 20.04 (CH_2), 32.05 (CH_2), 41.00 (CH_2), 45.23 (DMSO-CH_3), 45.38 (DMSO-CH_3), 114.00 (furan-*C*), 117.00 (furan-*C*), 119.00 (-*C*H=), 127.54 (-*C*H=), 144.00 (furan-*C*), 152.00 (furan-*C*), 153.88 (H-*C*=N) and 161.00 (*C*=O).

6.2. Biology

6.2.1. Trypanocidal in vitro test

Normal Assay. *Trypanosoma cruzi* epimastigotes (Tulahuen 2 strains) were grown at 28 °C in an axenic medium (BHI-Tryptose) as previously described [20–25], complemented with 5% fetal bovine serum. Cells from a 10-day old culture (stationary phase) were inoculated into 50 mL of fresh culture medium to give an initial concentration of 1×10^6 cells/mL. Cell growth was followed by measuring everyday the absorbance of the culture at 600 nm. Before inoculation, the media was added to the indicated amount of the drug from a stock solution in DMSO. The final concentration of DMSO in the culture media never exceeded 0.4% and the control was run in the presence of 0.4% DMSO and in the absence of any drug. No effect on epimastigotes growth was observed by the presence of up to 1% DMSO in the culture media. The percentage of inhibition was calculated as follows: $\%=\{1-[(A_p-A_{0p})/(A_c-A_{0c})]\}\times100$, where $A_p=A_{600}$ of the culture containing the drug at day 5; $A_{0p}=A_{600}$ of the culture containing the drug just after addition of the inocula (day 0); $A_c=A_{600}$ of the culture in the absence of any drug (control) at day 5; $A_{0c}=A_{600}$ in the absence of the drug at day 0.

Assay without proteins. *T. cruzi* epimastigotes (Tulahen 2 strain) from 5 days of growth were harvested by centrifugation (3000 rpm for 15 min), washed and resuspended in PBS-glucose (4 mL). The centrifugation was repeated (3000 rpm for 15 min), the supernatant discarded and the parasites re-suspended in PBS-glucose (4 mL). The indicated amount of the compound from a stock solution in DMSO was added and incubated for 5 h at 28 °C. Then, cells were harvested (3000 rpm for 15 min), supernatant discarded and the parasites re-suspended in an axenic medium (BHI-Tryptose) complemented with 5% fetal bovine serum. Afterwards, the procedure was continued in the same way as in the normal assay described above. The same procedure was performed for Nfx (reference drug) and vehicle alone, DMSO as blank.

6.3. Physicochemical properties

6.3.1. Stability studies

The stability studies were performed at 10^{-4} M complex concentration in a mixture of DMSO (0.5-1.0%):phosphate buffer (pH = 7.4). The solutions were kept at 28±1 °C and the variation of the spectrum in the range 300 – 800 nm was followed during 96 h with a Spectronic 3000 spectrophotometer. Conductimetric measurements were performed at 25 °C in 10^{-3} M water:DMSO (99.5:0.5) solutions using a Conductivity Meter 4310 Jenway.

6.3.2. Cyclic voltammetry

Cyclic voltammetry was carried out in DMSO (ca 1.0 mM) under nitrogen atmosphere at room temperature with $(TBA)PF_6$ (ca 0.1 mM) as supporting electrolyte, using a Metrohm 693 VA instrument with a 694 VA Stand convertor and a 693 VA Processor. A three electrodes cell was employed with a mercury-dropping electrode as working electrode, a platinum wire as auxiliary electrode, and a saturated calomel electrode as reference electrode.

6.3.3. P_{OW} determination

Lipophilicity tests were performed by the "shake flask" methodology determining the partition coefficient, P_{ow}, of the complexes in physiological solution/*n*-octanol. Concentration of Ru complexes in both phases was determined spectrophoto-

metrically by measuring the absorbance at the λ maximum of each complex [33].

6.3.4. Interaction with proteins

BSA (50 μM) and increased quantities of the metal complexes (2:1, 1:1, 0.5:1 ratios) were incubated al 37 °C in 100 mM phosphate buffer, pH 7.4. At different times, an aliquot of the incubated solutions was ultrafiltrated (Centrikon tubes, 10000 cut-off), and the amount of unbound complex was quantified by absorbance at the complex absorption maxima. The percentage of complex bound to BSA was determined by comparing the total amount of incubated complex with the unbound complex quantified after ultrafiltration.

The potential proteolitic activity of the metal complex was investigated incubating BSA and compound **7** at different molar ratios (1:0.1, 1:0.5 and 1:1) at 37 °C for 16 h. Protein hydrolysis was assayed on SDS-PAGE (10%) visualizing the proteic bands by Coomasie blue.

6.3.5. ESR experiments

NADPH, EDTA, DMPO and DMF were obtained from Sigma. Epimastigotes of *T. cruzi* (Brener strain) (7 mg protein/mL), NADPH (1 mM), EDTA (1 mM), DMPO (100 mM) in phosphate buffer pH 7.4 were incubated with the complexes (1 mM) dissolved in DMF. In all cases, NADPH was added immediately before the ESR spectrum was recorded. ESR spectra were recorded at 28 °C in the X band (9.68 GHz) using a Bruker ECS 106 spectrometer with a rectangular cavity and 50 kHz field modulation.

3.5.2. Oxygen uptake

Tulahuen strain *T. cruzi* epimastigotes were harvested by 500 × g centrifugation, followed by washing and resuspension in 0.05 M sodium phosphate buffer, pH 7.4, containing 0.107 M sodium chloride. Respiration measurements were carried out polarographically with a Clark N° 5331 electrode (Yellow Springs Instruments) in a 53 YSI model (Simpson Electric Co). The chamber volume was 2 mL and the temperature was 28 °C. The amount of parasite used was equivalent to 2 mg of protein. Parasite mass-drug ratio used in the oxygen uptake experiments was maintained as in the growth inhibition assays. Values are expressed as mean ± SD for three independent experiments.

Acknowledgements

This research has been supported by TWAS, Fondo Clemente Estable (Uruguay) and PEDECIBA (Uruguay). We thank a doctoral grant for L.O. from Programa de Desarrollo de Ciencias Básicas (PEDECIBA-Uruguay) and a scholarship from RTPD network.

References

[1] http://www.who.int/ctd/chagas.
[2] A. Moncayo, In *WHO Special Program for Research and Training in Tropical Diseases (TDR)*; World Health Organization Ed., Eleventh Programme Report of the UNPD: World Bank: Geneva, 1993: pp 67–75.
[3] W. De Souza, Curr. Pharm. Des. 4 (2002) 269–285.
[4] H. Cerecetto, M. González, Curr. Top. Med. Chem. 2 (2002) 1185–1211.
[5] J.A. Castro, E.G. Díaz de Toranzo, Biomed. Environ. Sci. 1 (1988) 19–33.
[6] N.B. Gorla, O.S. Ledesma, G.P. Barbieri, I.B. Larripa, Mutat. Res. 224 (1989) 263–267.
[7] B.K. Kepler, Metal complexes in cancer chemotherapy. General remarks, in: B. Kepler (Ed.), Metal complexes in Cancer Chemotherapy, VCH, Weinheim, 1993, pp. 1–7.
[8] G. Maestroni, E. Alessio, G. Sava, S. Pacor, M. Coluccia, The development of tumor-inhibiting ruthenium dimethylsulfoxide complexes, in: B. Kepler (Ed.), Metal Complexes in Cancer Chemotherapy, VCH, Weinheim, 1993, pp. 159–185.
[9] N. Farrell, in: Transition Metal Complexes as Drugs and Chemotherapeutic Agents, Vol 11, Kluwer Academic Publishers, London, 1989, pp. 230–232.
[10] R. Sánchez Delgado, A. Anzellotti, L. Suárez, Met. Ions. Biol. Sist. 41 (2004) 379–419.
[11] R. Sánchez Delgado, K. Lazardi, L. Rincón, J. Urbina, J. Med. Chem. 36 (1993) 2041–2043.
[12] R. Sánchez Delgado, M. Navarro, K. Lazardi, R. Atencio, M. Caparelli, F. Vargas, J. Urbina, A. Boulliez, A. Noels, D. Masi, Inorg. Chim. Acta 275-276 (1998) 528–540.
[13] M. Navarro, T. Lehman, E. Cisneros-Fajardo, A. Fuentes, R. Sánchez Delgado, J. Urbina, Polyhedron 19 (2000) 2319–2325.
[14] A.J. Castilla, C.M. Mesa-Valle, M. Sanchez Moreno, T. Arnedo, M. Rosales, C. Mascaro, D. Craciunescu, A. Osuna, Arzneim.-Forsch/Drug Res. 46 (1996) 990–996.
[15] C.M. Mesa-Valle, V. Moradela, D. Craciunescu, M.P. Alonso, A. Osuna, Arzneim.-Forsch/Drug Res. 43 (1993) 1010–1013.
[16] R.A. Sanchez-Delgado, M. Navarro, H. Perez, J.A. Urbina, J. Med. Chem. 39 (1996) 1095–1099.
[17] S. Singh, N. Bharti, M.T. Gonzalez Garza, D.E. Cruz-Vega, J. Castro Garza, K. Saleem, F. Naqvi, A. Azam, Bioorg. Med. Chem. Lett. 11 (2001) 2675–2678.
[18] S. Singh, N. Bharti, F. Naqvi, A. Azam, Bioorg. Med. Chem. Lett. 13 (2003) 689–692.
[19] S. Singh, N. Bharti, F. Naqvi, A. Azam, Eur. J. Med. Chem. 39 (2004) 459–465.
[20] H. Cerecetto, R. Di Maio, G. Ibarruri, G. Seoane, A. Denicola, G. Peluffo, C. Quijano, M. Paulino, Farmaco 53 (1998) 89–94.
[21] R. Di Maio, H. Cerecetto, G. Seoane, C. Ochoa, V.J. Arán, E. Pérez, A. Gómez, S. Muelas, A.R. Martínez, Arzneimittel Fors. Drug Res. 49 (1999) 759–763.
[22] H. Cerecetto, R. Di Maio, M. González, M. Risso, G. Sagrera, G. Seoane, A. Denicola, G. Peluffo, C. Quijano, M.A. Basombrío, A.O.M. Stoppani, M. Paulino, C. Olea-Azar, Eur. J. Med. Chem. 35 (2000) 343–350.
[23] S. Muelas, R. Di Maio, H. Cerecetto, G. Seoane, C. Ochoa, J.A. Escario, A. Gómez-Barrio, Folia Parasit. 48 (2001) 105–108.
[24] G. Aguirre, E. Cabrera, H. Cerecetto, R. Di Maio, M. González, G. Seoane, A. Duffaut, A. Denicola, M.J. Gil, V. Martínez-Merino, Eur. J. Med. Chem. 39 (2004) 421–431.
[25] G. Aguirre, H. Cerecetto, M. González, D. Gambino, L. Otero, C. Olea-Azar, C. Rigol, A. Denicola, Bioorg. Med. Chem. 12 (2004) 4885–4893.
[26] L. Otero, P. Noblia, D. Gambino, H. Cerecetto, M. González, R. Sánchez Delgado, E.E. Castellano, O.E. Piro, Anorg. Allg. Chem 629 (2003) 1033–1038.
[27] L. Otero, P. Noblia, D. Gambino, H. Cerecetto, M. González, R. Di Maio, J. Ellena, O.E. Piro, Inorg. Chim. Acta 344 (2003) 85–94.

[28] G. Aguirre, M. Boiani, E. Cabrera, H. Cerecetto, R. Di Maio, M. González, A. Denicola, C.M.R. Sant'Anna, E.J. Barreiro, New potent 5-nitrofuryl derivatives as inhibitors of Trypanosoma cruzi growth-3D-QSAR (COMFA) studies, Eur. J. Med. Chem 41 (2006) 457–466 (in press).
[29] J. Chatt, G.A. Rowe, J. Chem. Soc. (1962) 4019–4025.
[30] I. Evans, A. Spencer, G. Wilkinson, J. Chem. Soc., Dalton Trans. (1973) 204–209.
[31] A. Denicola, H. Rubbo, D. Rodríguez, R. Radi, Arch. Biochem. Biophys. 304 (1993) 279–286.
[32] E. Cabrera, H. Cerecetto, M. González, D. Gambino, P. Noblia, L. Otero, B. Parajón-Costa, A. Anzillotti, R. Sánchez-Delgado, A. Azqueta, A. López de Ceráin, A. Monge, Eur. J. Med. Chem. 39 (2004) 377–382.
[33] A. Leo, C. Hansch, D. Elkins, Chem. Rev. 71 (1971) 525–554.
[34] C.A. Lipinski, F. Lombardo, B.W. Dominy, P.J. Feeney, Adv. Drug Deliv. Rev. 23 (1997) 3–25.
[35] C. Olea-Azar, C. Rigol, F. Mendizabal, A. Morello, J.D. Maya, C. Moncada, E. Cabrera, R. Di Maio, M. González, H. Cerecetto, Free Rad. Res. 37 (2003) 993–1001.
[36] C. Lai, T.A. Grover, L.H. Piette, Arch. Biochem. Biophys. 193 (1979) 373–378.
[37] S.N.J. Moreno, J. Schreiber, R.P. Mason, J. Biol. Chem. 261 (1986) 7811–7815.
[38] J.D. Maya, S. Bollo, L.J. Núñez-Vergara, J.A. Squella, Y. Repetto, A. Morello, J. Périé, G. Chauvière, Biochem. Pharmacol. 65 (2003) 999–1006.
[39] C. Olea-Azar, A.M. Atria, R. Di Maio, G. Seoane, H. Cerecetto, Spectrosc. Lett. 31 (1998) 849–857.
[40] L. Messori, P. Orioli, D. Vullo, E. Alessio, E. Lengo, Eur. J. Biochem. 267 (2000) 1206–1213.